# Theoretical model analysis of $(d,xn)$ reactions on $^9$Be and $^{12}$C at incident energies up to 50 MeV

Shinsuke Nakayama,[1,*] Hiroshi Kouno,[2] Yukinobu Watanabe,[2] Osamu Iwamoto,[1] and Kazuyuki Ogata[3]

[1]*Nuclear Data Center, Japan Atomic Energy Agency, Ibaraki 319-1195, Japan*
[2]*Department of Advanced Energy Engineering Science, Kyushu University, Fukuoka 816-8580, Japan*
[3]*Research Center for Nuclear Physics, Osaka University, Osaka 567-0047, Japan*

**Background:** In the design of deuteron accelerator neutron sources, accurate nuclear data of deuteron-induced reactions are indispensable over a wide range of incident energy. Reliable model calculations play an important role in completing the necessary nuclear data since currently available experimental data are insufficient. We have been developing a code system dedicated for the deuteron-induced reactions, called deuteron-induced reaction analysis code system (DEURACS). It was applied successfully to $(d,xp)$ reactions at 56 and 100 MeV.

**Purpose:** The purpose of the present work is to investigate the applicability of DEURACS to $(d,xn)$ reactions on $^9$Be and $^{12}$C for incident energies below 50 MeV and to clarify neutron production mechanism.

**Methods:** Double-differential thick target neutron yields (TTNYs) from deuteron bombardment on thick Be and C targets are analyzed. The TTNYs are derived using the double differential $(d,xn)$ cross sections calculated by DEURACS and the stopping power of deuteron in the target. The calculated TTNYs are decomposed into individual components corresponding to elastic breakup, proton stripping, and statistical decay reactions.

**Results:** The calculated TTNYs reproduced the experimental data quantitatively well in the incident energy range up to 50 MeV. From the analysis, it was found that the proton stripping reaction makes the most dominant contribution to neutron production.

**Conclusions:** DEURACS is applicable to $(d,xn)$ reactions on $^9$Be and $^{12}$C for incident energies below 50 MeV. Modeling of the stripping reaction is essential to predict neutron production yields accurately in the design of deuteron accelerator neutron sources.

## I. INTRODUCTION

In recent years, intensive neutron sources using deuteron accelerators have been proposed for various applications such as the International Fusion Materials Irradiation Facility (IFMIF) [1] and Neutron For Science (NFS) in SPIRAL2 [2], and also medical applications such as boron neutron capture therapy (BNCT) [3] and production of radioisotopes for medical use [4,5]. In these facilities, $(d,xn)$ reactions on such light elements as Li, Be, and C are used to generate intense neutron beams. The neutron spectrum generated by the $(d,xn)$ reaction has a broad energy peak around half the deuteron incident energy. This means that the most probable energy of the generated neutron can be selected by adjusting the incident deuteron energy. Therefore, accurate nuclear data of deuteron-induced reactions over a wide range of incident energies are indispensable for the design of deuteron accelerator neutron sources. However, currently available experimental data of deuteron-induced reactions are not necessarily enough for the requirement. In such a case, theoretical model calculations play a key role in completing the necessary nuclear data by interpolation and extrapolation of experimental data.

Double-differential cross sections (DDXs) of $(d,xn)$ reactions are critically important in the design of neutron sources but there are few experimental DDX data of $(d,xn)$ reactions. On the other hand, experimental DDX data of $(d,xp)$ reactions and double-differential thick-target neutron yields (TTNYs)

from deuteron bombardment on thick targets exist to some extent. Instead of DDXs of $(d,xn)$ reactions, these data are useful to investigate the applicability of theoretical models to deuteron-induced reactions.

Recently, Hashimoto *et al.* developed an approach to describe $(d,xn)$ reactions by combining the Intra-Nuclear Cascade of Liège (INCL) [6] and distorted wave Born approximation (DWBA). They have implemented the method in the particle and heavy ion transport code system (PHITS) [7], a Monte Carlo simulation code, and applied it to the analysis of TTNYs [8]. However, it is necessary to validate the applicability of the INC-based method to deuteron-induced reactions at low incident energies below a few tens of MeV. On the other hand, Wei *et al.* have performed the analysis of TTNYs from $^9$Be$(d,xn)$ reactions in the incident deuteron energy range up to 20 MeV [9]. In their analysis, the TALYS code [10] was adopted to calculate DDXs of $^9$Be$(d,xn)$ reactions and a series of model parameters were optimized to reproduce experimental data well. Therefore, it is controversial whether their model calculation works well for incident energies larger than 20 MeV or target nuclei other than $^9$Be. Furthermore, quantitative relations among the individual reaction components responsible for neutron production were not sufficiently clarified in their work.

Under the above situation, we have been developing a code system dedicated for deuteron-induced reactions, called the deuteron-induced reaction analysis code system (DEURACS) [11–14]. DEURACS consists of several calculation codes based on theoretical models to describe respective reaction mechanisms. In the development of DEURACS, we have

*nakayama.shinsuke@jaea.go.jp

adopted theoretical models which require as few adjustable parameters as possible. In our early works [12,13], DEURACS had been successfully applied to systematic analyses of DDXs of the $(d,xp)$ reactions for $^{12}$C, $^{27}$Al, and $^{58}$Ni at two incident energies of 56 and 100 MeV where experimental data are available. The calculation result was in good agreement with the experimental data. Note that similar analyses of inclusive $(d,xp)$ reactions have recently been reported with particular attention to inclusive deuteron breakup by other research groups [15–17].

As our next step, it is interesting to investigate the applicability of DEURACS to $(d,xn)$ reactions on such light nuclei as $^9$Be and $^{12}$C in a wide incident energy range and to clarify the neutron production mechanism. As mentioned above, experimental DDXs of $(d,xn)$ reactions are very limited, while the measured TTNY data of $^9$Be and $^{12}$C are available in the incident energy range up to 50 MeV. Therefore, we derive TTNYs from the DDXs calculated with DEURACS and discuss the neutron production mechanism through comparisons of the calculated TTNYs with the measured data.

Section II describes a method of calculating TTNYs from DDXs and theoretical reaction models implemented in DEURACS. Input parameters used in model calculations are also explained here. In Sec. III, calculation results are compared with experimental data and discussed. Finally, a summary and conclusion are given in Sec. IV.

## II. MODELS AND METHODS

### A. Calculation method of thick target neutron yield

To calculate TTNYs from DDXs, we use the following expression under the assumption that multiple scattering of incident deuterons and emitted neutrons in the target is ignored:

$$\frac{d^2Y}{dEd\Omega}(E_{in}) = \int_0^{E_{in}} dE_d N \frac{d^2\sigma_{(d,xn)}}{dEd\Omega}(E_d)\left[\frac{dE}{dx}(E_d)\right]^{-1} D(E_d),$$
(1)

where $E_{in}$ is the incident deuteron energy, $N$ is the atomic density of the target material, $E_d$ is the deuteron energy in the target, $d^2\sigma_{(d,xn)}/(dEd\Omega)$ is the DDXs of $(d,xn)$ reactions, and $dE/dx$ is the deuteron stopping power. The attenuation rate of the incident deuteron flux, $D$, is given as

$$D(E_d) = \exp\left[-\int_{E_d}^{E_{in}} dE' N\sigma_r(E')\left[\frac{dE}{dx}(E')\right]^{-1}\right], \quad (2)$$

where $\sigma_r$ is the deuteron total reaction cross section.

We calculate the stopping power and the total reaction cross section with the SRIM-2010 code [18] and the optical model implemented in the CCONE code [19,20], respectively. The DDXs of the $(d,xn)$ reaction are calculated using DEURACS in the same manner as in Refs. [12,13]. In DEURACS, DDXs of $(d,xn)$ reactions are expressed by incoherent summation of three components:

$$\frac{d^2\sigma_{(d,xn)}}{dEd\Omega} = \frac{d^2\sigma_{EB}}{dEd\Omega} + \frac{d^2\sigma_{p-STR}}{dEd\Omega} + \frac{d^2\sigma_{SD}}{dEd\Omega}, \quad (3)$$

where $d^2\sigma_{EB}/(dEd\Omega)$, $d^2\sigma_{p-STR}/(dEd\Omega)$, and $d^2\sigma_{SD}/(dEd\Omega)$ correspond to the DDXs for elastic breakup reaction, proton stripping reaction, and statistical decay, respectively.

First, among these three DDXs, the elastic breakup component is directly calculated with the calculation code based on the continuum-discretized coupled-channels method (CDCC) [21].

Second, the proton stripping component is divided into two terms, namely the DDXs for stripping reactions to continuum and to discrete levels. The former one is calculated by the Glauber model as described in Refs. [22,23]. In the present work, a noneikonal approach is incorporated into the Glauber model as in Ref. [23]. Namely, the eikonal $S$ matrices used in the Glauber model are replaced by the quantum $S$ matrices given by the optical model calculations with the ECIS-96 code [24]. Next, the DDXs for transition to discrete levels are obtained by folding the calculated DWBA cross section corresponding to each discrete level with a Gaussian function to reproduce the experimental energy resolution. We employ the zero-range DWBA code DWUCK4 [25] for the DWBA calculation. It should be noted that the Glauber model cannot deal with individual transitions to discrete levels by stripping process and calculates the sum of stripping to both continuum and bound states as a continuous spectrum. Therefore, the DDXs calculated by the Glauber model and the DWBA approach overlap with each other in the energy region corresponding to the transitions to discrete levels. To avoid double counting, we cutoff the DDXs calculated by the Glauber model in this energy region. The remaining Glauber model component is normalized so that the total stripping cross section calculated by the Glauber model is conserved.

Third, the statistical decay component is calculated using the method based on the exciton and Hauser-Feshbach models implemented in the CCONE code [19,20], which was successfully applied to calculation of neutron induced reactions for the latest version of the Japanese Evaluated Nuclear Data Library (JENDL-4.0) [26]. In the calculation, three different compound nuclei are considered because they can be formed by absorption of either a neutron or a proton in the incident deuteron or the deuteron itself. Therefore, the DDXs for the statistical decay are calculated in the following way:

$$\frac{d^2\sigma_{SD}}{dEd\Omega} = R_d\frac{d^2\sigma_{(d,xn)}^{CCONE}}{dEd\Omega} + R_p\frac{d^2\sigma_{(p,xn)}^{CCONE}}{dEd\Omega} + R_n\frac{d^2\sigma_{(n,xn)}^{CCONE}}{dEd\Omega} \quad (4)$$

where $R_d$, $R_p$, and $R_n$ denote the formation fractions of three different compound nuclei, which are calculated with the Glauber model, and $d^2\sigma_{(d,xn)}^{CCONE}/(dEd\Omega)$, $d^2\sigma_{(p,xn)}^{CCONE}/(dEd\Omega)$, $d^2\sigma_{(n,xn)}^{CCONE}/(dEd\Omega)$ are the DDXs of $(d,xn)$, $(p,xn)$, and $(n,xn)$ reactions calculated with the CCONE code, respectively.

In the calculation of $(p,xn)$ and $(n,xn)$ components in Eq. (4), we assume that the incident energies of the proton and the neutron are half the deuteron incident energy for saving the computational time. Indeed, the proton or the neutron absorbed in the target nucleus by the stripping reaction has a certain energy distribution. Therefore, some differences are seen between the components by proton or neutron absorption of this approximate case and those of the case where energy distribution is considered properly. However, we confirmed

that there is not a significant difference between the summed DDXs for the statistical decay of the two cases, because the component by complete deuteron absorption, i.e., the first term in the right-hand side of Eq. (4), is dominant over those by nucleon absorption at incident energies considered in the present work. Note that some differences might appear in the calculation of production cross sections of evaporation residues although it is not the object of the present work.

Finally, the substitution of Eq. (3) into Eq. (1) yields the following incoherent sum of each component for the TTNYs:

$$\frac{d^2Y}{dEd\Omega} = \frac{d^2Y_{EB}}{dEd\Omega} + \frac{d^2Y_{p-STR}}{dEd\Omega} + \frac{d^2Y_{SD}}{dEd\Omega}. \quad (5)$$

Thus, we can analyze the relative contribution of individual reaction processes to deuteron-induced neutron production by comparing the calculated TTNYs with the experimental one.

### B. Input parameters of model calculations

The calculation models integrated in DEURACS use some input parameters. In the CDCC method and the Glauber model, nucleon optical potentials (OPs) at half the incident deuteron energy are necessary. There is no global nucleon OP for $^9$Be and $^{12}$C applicable to wide incident range from a few MeV to several tens of MeV. A systematic study of nucleon OPs for $1p$-shell nuclei was performed by Watson *et al.* [27], but their nucleon OPs are limited to incident energies between 10 and 50 MeV. On the other hand, the global nucleon OPs derived by Koning and Delaroche (K-D) [28] are widely used in the incident energy range from 1 keV to 200 MeV, but the lower limit of target mass range is $A = 24$. Since preliminary calculations with the K-D and Watson OPs show only about 10% differences between them in the energy range where the Watson OPs are valid, we have chosen the K-D OPs for both neutron and proton from the viewpoint of applicable energy range.

Next, the input parameters used in the DWUCK4 calculation are summarized in Table I. These parameters are the same as those used in the systematic $(d, p)$ analysis [13]. We use the adiabatic potential [29] based on the nucleon OPs of K-D for deuteron. The adiabatic potential includes the effects of the deuteron breakup in the mean field of the target and it requires only the nucleon OPs. It should be noted that the validity and effectiveness of deuteron potential based on the adiabatic approximation has been examined in Ref. [30].

Finally, in the CCONE calculation, the An and Cai (An-Cai) global OPs [31] and the K-D OPs are used for the deuteron OPs and the nucleon OPs, respectively. For the level-density parametrization, we use the systematics of Mengoni and Nakajima [32]. The discrete levels are taken from the Reference Input Parameter Library (RIPL) database [33]. Default values in the CCONE code are employed for other input parameters.

## III. RESULTS AND DISCUSSION

### A. Stripping reactions to discrete levels

Proton stripping reactions to discrete levels are expected to make a large contribution to neutron production especially in the high emission energy region. Generally, a conventional DWBA calculation of nucleon stripping reactions requires the spectroscopic factors (SFs) for single nucleon orbits. As mentioned in Refs. [34,35], large discrepancies are often seen for the SF values reported in the experimental literatures. This is mainly due to the difference in such input parameters as optical potentials used in the DWBA analyses. In the present work, therefore, we perform a consistent DWBA analysis of all available experimental data using the same input parameters listed in Table I in order to extract the SFs corresponding to individual discrete levels in $^{10}$B and $^{13}$N of the residual nuclei.

#### 1. DWBA analysis

In the DWBA analysis for the $^9$Be$(d,n)^{10}$B and $^{12}$C$(d,n)^{13}$N reactions, we consider eight levels of $^{10}$B and four levels of $^{13}$N where experimental differential cross sections are available [36–42]. Some quantities corresponding to these levels, namely the excitation energy $E_x$, the spin-parity $J^\pi$, and the angular momentum transfer $l$ are summarized in Table II. The SFs are extracted by fitting the calculated DWBA cross section to the corresponding experimental cross section at

TABLE I. Input parameters used in the DWUCK4 calculation.

| | |
|---|---|
| Neutron potential | Koning-Deraloche (K-D) [28] |
| Deuteron potential | Adiabatic potential [29] from K-D |
| Proton binding potential | Woods-Saxon form |
| | $r_0 = 1.25$ [fm], $a_0 = 0.65$ [fm] |
| Finite range correction factor [fm] | 0.7457 |
| Zero range constant $D_0$ [MeV$^2$fm$^3$] | $1.5 \times 10^4$ |
| Nonlocality parameters | neutron:0.85, deuteron:0.54 |

TABLE II. Discrete levels of the residual nuclei, $^{10}$B and $^{13}$N, considered in the present analysis. $F_i$ denote the scaling factors for $S(E_d)$ derived in Ref. [13] (see Sec. III A 2).

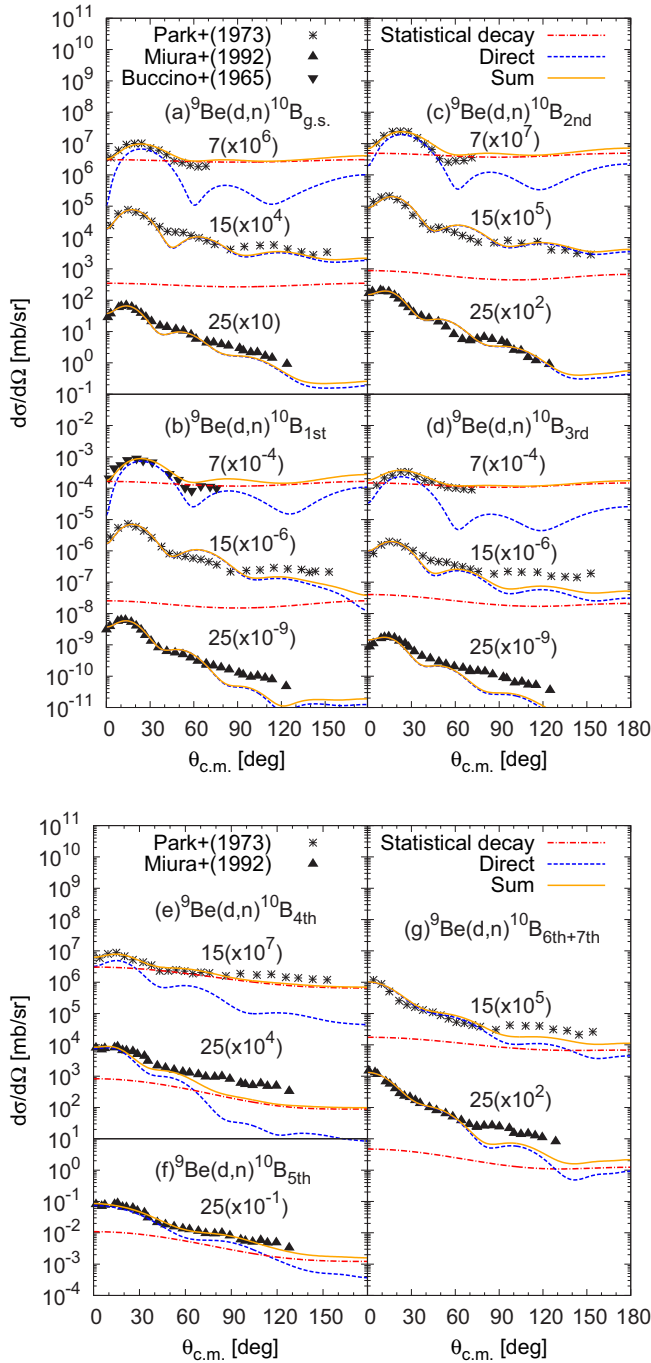| | $i$ | $E_x$(MeV) | $J^\pi$ | $l$ | $F_i$ |
|---|---|---|---|---|---|
| $^9$Be$(d,n)^{10}$B | 0 | 0(g.s.) | $3^+$ | 1 | 1.14 |
| | 1 | 0.72 | $1^+$ | 1 | 2.12 |
| | 2 | 1.74 | $0^+$ | 1 | 0.24 |
| | 3 | 2.15 | $1^+$ | 1 | 0.22 |
| | 4 | 3.59 | $2^+$ | 1 | 0.14 |
| | 5 | 4.77 | $3^+$ | 3 | 0.05 |
| | 6 | 5.11 | $2^-$ | 0 | 0.21 |
| | 7 | 5.16 | $2^+$ | 1 | 0.63 |
| $^{12}$C$(d,n)^{13}$N | 0 | 0(g.s.) | $\frac{1}{2}^-$ | 1 | 1.00 |
| | 1 | 2.37 | $\frac{1}{2}^+$ | 0 | 0.76 |
| | 2 | 3.51 | $\frac{3}{2}^-$ | 1 | 0.23 |
| | 3 | 3.55 | $\frac{5}{2}^+$ | 2 | 0.97 |

FIG. 1. Calculated and experimental differential cross sections for the $^9$Be$(d,n)^{10}$B reaction. The short-dashed and dash-dotted curves represent the direct stripping component calculated by DWBA and the statistical decay contribution from compound nuclei calculated with the CCONE code, respectively. The solid curves are the sum of them. The number at the top of each plot denotes incident energy in MeV.



FIG. 2. Same as Fig. 1 but for the $^{12}$C$(d,n)^{13}$N reaction.

$^9$Be$(d,n)^{10}$B reaction in the incident energy range from 7 to 25 MeV. The experimental data are taken from Refs. [36–38]. Since the experimental values for the sixth and the seventh excited levels are unresolved, the ratio of the SFs between the sixth level and the seventh level is assumed to be 1 to 3 as given in Ref. [37]. The sum of the direct stripping component calculated by DWBA and contribution from statistical decay show good agreement with the experimental data over a wide range of emission angle.

In Fig. 2, some typical results for the $^{12}$C$(d,n)^{13}$N reaction are shown in the incident energy range from 7 to 18 MeV. The experimental data are taken from Refs. [39–42]. It should be noted that the excited states of $^{13}$N are unbound since the proton separation energy of $^{13}$N is 1.94 MeV. Following Ref. [40], we calculate the DWBA cross section for these states using a very loosely bound state wave function by setting the binding energy to 0.01 MeV. In addition, the experimental values for the second and third excited levels are unresolved. From the previous analysis of the transition to isobaric analog states of $^{13}$N via the $^{12}$C$(d,p)^{13}$C reaction [13], we evaluate the SF values for the third excited level which is four times as large as that for the second excited level. Similarly to Fig. 1, the calculations reproduce the experimental data well at forward angles.

### 2. Evaluation of spectroscopic factors

The experimental SFs for the $^9$Be$(d,n)^{10}$B and $^{12}$C$(d,n)^{13}$N reactions extracted from the present analysis are plotted by closed and open circles in Fig. 3. The dependence of the

forward angles where the proton stripping process is dominant. The statistical decay contribution from compound nuclei is estimated by calculation with the CCONE code.

Figure 1 shows some examples of comparison between calculated and experimental differential cross sections for the
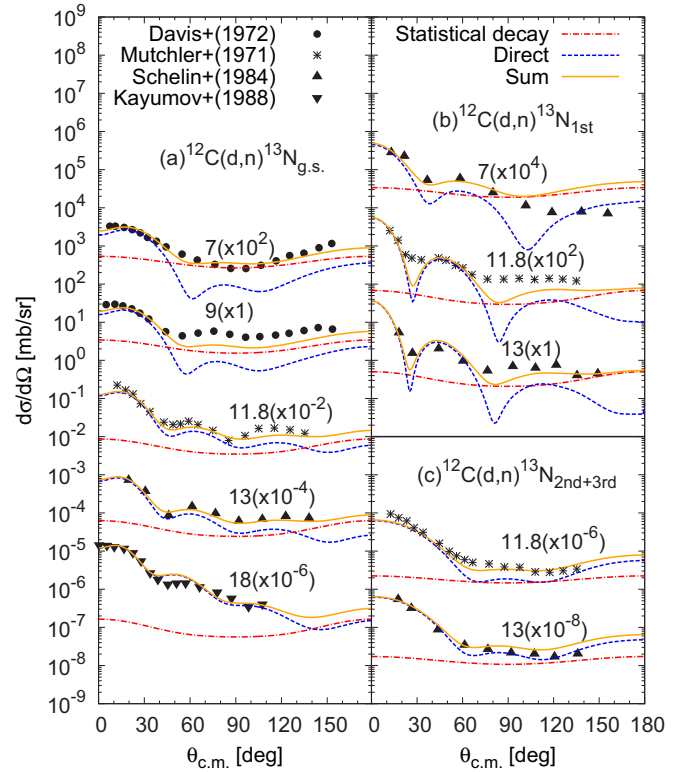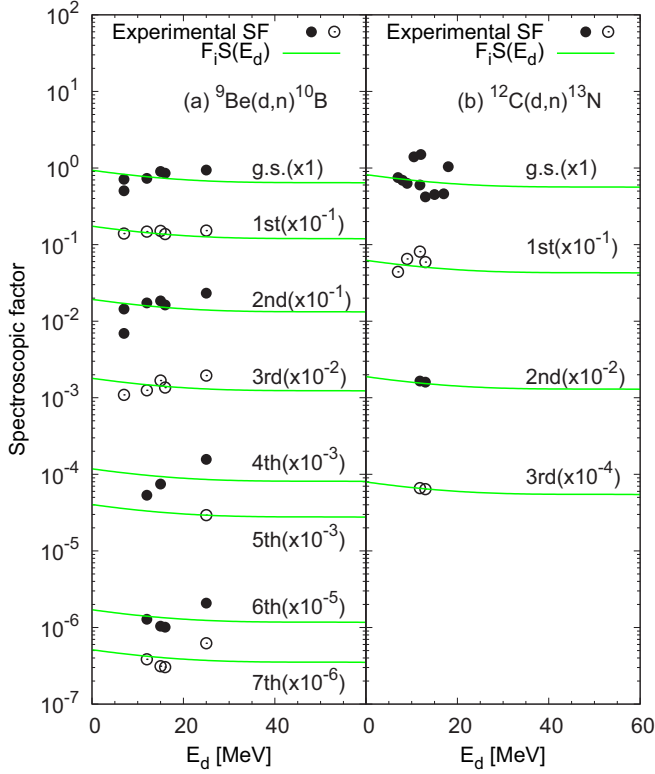
FIG. 3. Experimental and empirical spectroscopic factors for (a) $^9\mathrm{Be}(d,n)^{10}\mathrm{B}$ and (b) $^{12}\mathrm{C}(d,n)^{13}\mathrm{N}$ reactions. The solid curves represent the products of $F_i$ in Table II and $S(E_d)$ given by Eq. (6) for individual $i$th levels of the residual nuclei. Experimental spectroscopic factors are plotted by closed or open circles.

experimental SFs on incident energy is not necessarily smooth. The fluctuation seen in the figure is likely to be due to the effect of resonance structures as pointed out in Ref. [39].

In the previous DWBA analyses for the $(d,p)$ reactions on $^{12}\mathrm{C}$, $^{27}\mathrm{Al}$, $^{40}\mathrm{Ca}$, and $^{58}\mathrm{Ni}$ for incident energies up to 100 MeV [13], we have found that the extracted SFs for transition to the ground state have a weak incident energy dependence and the trend is very similar among the target nuclei. The SF for the $^{12}\mathrm{C}(d,p)^{13}\mathrm{C}_{\mathrm{g.s.}}$ reaction is given as a function of incident energy $E_d$ by the following empirical expression [13]:

$$S(E_d) = -2.18 \times 10^{-6} E_d{}^3 + 3.19 \times 10^{-4} E_d{}^2$$
$$- 1.56 \times 10^{-2} E_d + 8.20 \times 10^{-1}. \quad (6)$$

In the present work, we assume that the SFs for $^9\mathrm{Be}(d,n)^{10}\mathrm{B}$ and $^{12}\mathrm{C}(d,n)^{13}\mathrm{N}$ reactions have the same energy dependence as the empirical $S(E_d)$ given by Eq. (6). Since the $S(E_d)$ is determined for the $^{12}\mathrm{C}(d,p)^{13}\mathrm{C}_{\mathrm{g.s.}}$ reaction, it is necessary to introduce a scaling factor $F_i$ depending on each $i$th level of the residual nuclei. We have averaged the fluctuation seen in Fig. 3 and determined each $F_i$ as follows. For the $^9\mathrm{Be}(d,n)^{10}\mathrm{B}$ reaction, we determine each $F_i$ so that $F_i S(E_d)$ passes through the center of the experimental SFs. For the $^{12}\mathrm{C}(d,n)^{13}\mathrm{N}$ reaction, $F_i$ of the second and the third excited levels of $^{13}\mathrm{N}$ are determined in the same manner as for the $^9\mathrm{Be}(d,n)^{10}\mathrm{B}$ reaction. On the other hand, for the ground and the first excited levels of $^{13}\mathrm{N}$, we adopt the same $F_i$ as the ones for the cor-
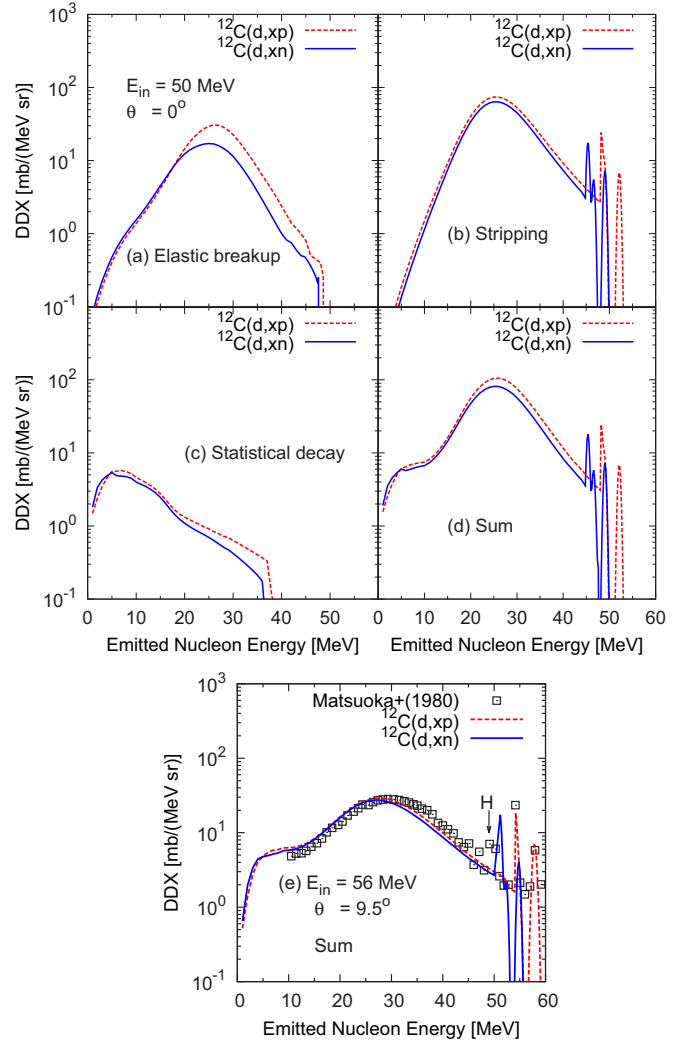


FIG. 4. Calculated DDXs for the $^{12}\mathrm{C}(d,xn)$ and the $^{12}\mathrm{C}(d,xp)$ reactions at the incident energy of 50 MeV. The components of elastic breakup (a), stripping (b), and statistical decay (c), and the sum of each component (d) are shown, respectively. In (e), the experimental $^{12}\mathrm{C}(d,xp)$ spectrum for $9.5^\circ$ at 56 MeV is compared with the calculated $(d,xp)$ and $(d,xn)$ spectra. "H" denotes the effect of hydrogen contamination.

responding states of $^{13}\mathrm{C}$ derived in Ref. [13]. The determined scaling factors $F_i$ are listed in Table II. The empirical SFs given by $F_i S(E_d)$ are shown by solid curves in Fig. 3, which are used in the DWBA calculation in Secs. III B and III C.

### B. Double differential cross section

We present the DDXs calculated using DEURACS with the parameters described in Sec. II. As mentioned in Sec. I, there are no available experimental DDX data for $(d,xn)$ reactions of interest. Therefore, we compare the calculated DDXs of the $^{12}\mathrm{C}(d,xn)$ reaction with those of the $^{12}\mathrm{C}(d,xp)$ reactions to which DEURACS was successfully applied [13]. The result is shown for the emission angle of $0^\circ$ and incident energy of 50 MeV in Fig. 4. Individual panels in the figure show the contributions from three different reaction processes and the

sum of them. An appreciable difference is seen between the $(d,xn)$ and $(d,xp)$ reactions in the elastic breakup component (a). The difference can be explained by the Coulomb breakup from our preliminary analysis in which both elastic breakup components are equal if only the nuclear breakup is taken into account. On the other hand, there are not significantly large differences between the $(d,xn)$ and $(d,xp)$ reactions with respect to the stripping component (b) and the statistical decay one (c). As mentioned in Ref. [43], the effect of Coulomb interaction in the stripping reactions is small. Sharp peaks seen around the high emission energy end in panel (b) correspond to the transition to discrete levels by the stripping reaction. These peak positions are different between the $(d,xn)$ and $(d,xp)$ reactions. This is because both the reactions excite different levels in the residual nuclei and the $Q$ values for each transition are different. The summed spectra (d) are nearly equal between neutron and proton emissions to the continuum as the relative contribution of the elastic breakup component is smaller than that of the nucleon stripping component.

In Fig. 4(e), the experimental $^{12}$C$(d,xp)$ spectrum for 9.5° at 56 MeV [44] is compared with the calculated $(d,xp)$ and $(d,xn)$ spectra. Since the DEURACS calculation provides good agreement with the experimental $(d,xp)$ data, it is expected that DEURACS can yield reasonable DDXs for the $(d,xn)$ reactions. In the next subsection, analyses of experimental TTNY data will be shown to investigate the applicability of DEURACS to $(d,xn)$ reactions at incident energies below 50 MeV.

### C. Thick target neutron yield

TTNYs on $^9$Be and $^{12}$C calculated using Eq. (1) are compared with available experimental data at incident energies up to 50 MeV and the reaction mechanism of deuteron-induced neutron production is discussed.

Figures 5 and 6 show comparisons between the calculated and experimental TTNYs on $^9$Be and $^{12}$C targets at angles around 0°, respectively. The experimental data are taken from Refs. [45–55]. The calculated TTNYs are decomposed to the three components expressed in Eq. (5) and each component is also shown in the figures. The calculation reproduces both the shape and magnitude of the experimental TTNY data in the wide incident energy range up to 50 MeV. As shown in the figures, the proton stripping process is found to be the most dominant at any incident energies. In our previous $(d,xp)$ analyses [12,13], the DEURACS calculations have shown that the neutron stripping process is the most dominant in forward proton emission at incident energies of 56 and 100 MeV. Thus, it is suggested that the stripping processes make the most dominant contribution to nucleon emission in the incident energy range below 100 MeV.

In the present analysis, we have adopted the semiclassical Glauber model to describe the stripping reaction to continuum. The bump structure seen around half the incident energy is described well by the Glauber model calculation in Figs. 5 and 6. Thus, the Glauber model seems to work well at low incident energies even though the model is based on the eikonal and adiabatic approximations. The applicability of the Glauber model to relatively low incident energy is supported by the
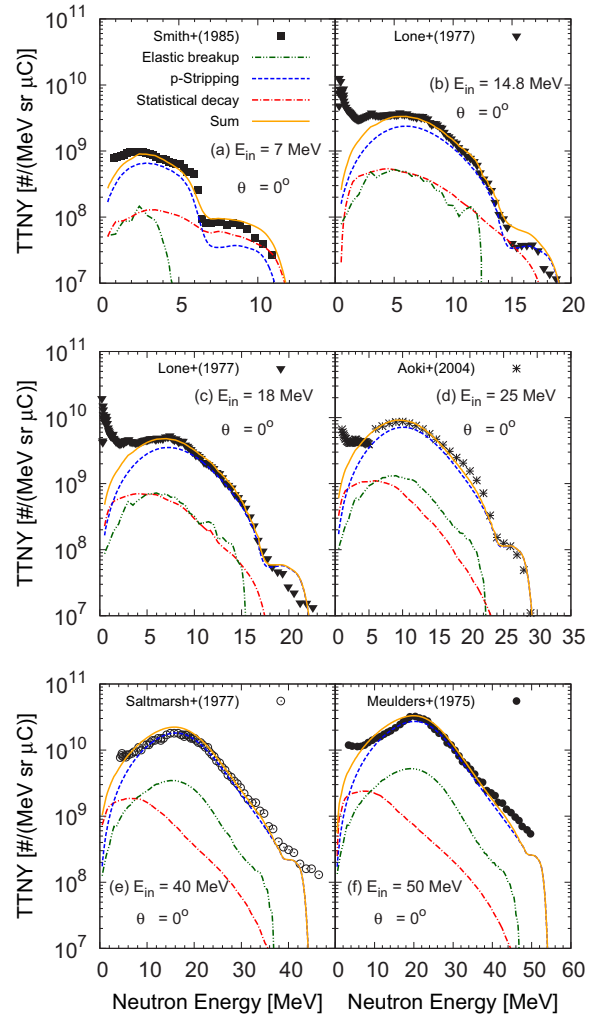


FIG. 5. Calculated and experimental TTNYs for the $^9$Be$(d,xn)$ reactions at 0°. The dash-dot-dotted, the short-dashed, and the dash-dotted curves represent the component of elastic breakup, proton stripping, and statistical decay, respectively. The solid curves are sums of each component.

previous analysis [22], in which it was clarified that the major contribution of the stripping reaction comes from the peripheral region of target nucleus and the potential depth in the region is sufficiently shallower than the incident energy. Also, a characteristic step-like structure is seen in the high emission energy region, especially in TTNYs at incident energies below 25 MeV. This high-energy component is formed by the stripping reaction to discrete levels in the residual nuclei. This component is described by the DWBA calculation with the incident energy dependent SFs instead of the Glauber model calculation. Therefore, the DWBA calculation plays an essential role in reproducing neutron emission spectra in the high emission energy region, particularly for relatively low incident energies.

Figure 7 shows the comparisons between the calculated and experimental TTNYs at several forward angles up to 40°. The experimental data are taken from Refs. [47,51]. For comparison, we also present the TTNYs calculated with the PHITS code [7] in which the INCL-DWBA approach [8] is
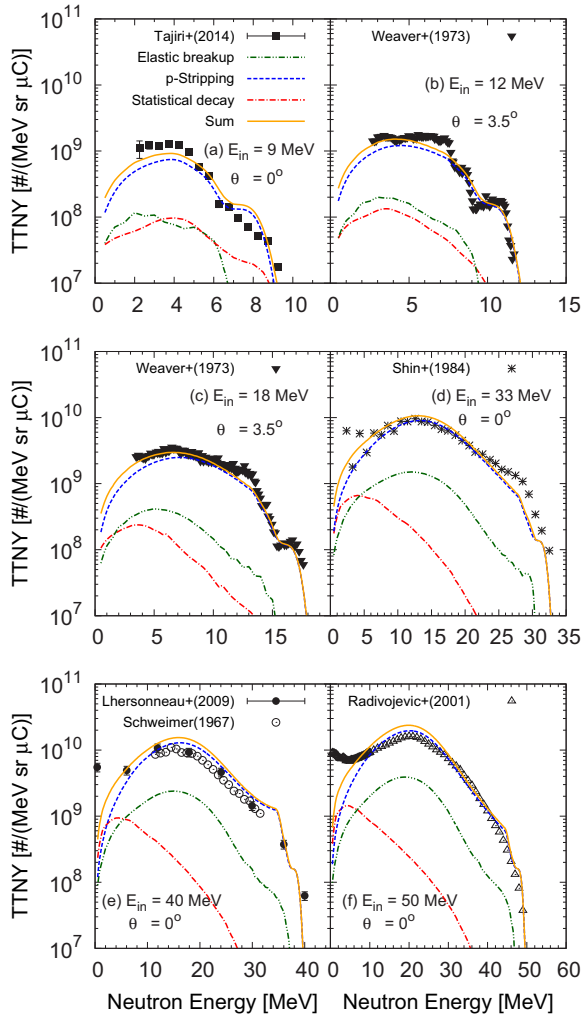
FIG. 6. Same as Fig. 5 but for the $^{12}$C$(d,xn)$ reactions at angles around $0°$.



FIG. 7. Calculated and experimental TTNYs at several angles for (a) the $^9$Be$(d,xn)$ reactions and (b) the $^{12}$C$(d,xn)$ reactions. The solid curves represent the TTNYs derived from the DEURACS calculation. The dashed lines are results of the Monte Carlo simulation codes PHITS.

employed. It should be noted that the transport of produced neutrons in the target is simulated in the PHITS calculation, namely neutron multiple scattering can be considered in a Monte Carlo method. The DEURACS calculation is in generally better agreement than the PHITS calculation in the whole angular range. Especially, a distinct difference between both calculations is seen in the broad peak around half the deuteron incident energy. This indicates that the INCL model [6] used in the PHITS code fails to reproduce the proton stripping process to continuum at relatively low incident energies.

Another difference between the two calculations appears in the low emission energy region, where the DEURACS calculation underestimates the TTNY spectra especially in the case of the $^9$Be$(d,xn)$ reaction. The same trend is seen in Figs. 5 and 6. The PHITS calculation reproduces the low energy component better than the DEURACS calculation, although the former still underestimates the experimental $^9$Be$(d,xn)$ data in a few MeV emission energy region. The absence of neutron multiple scattering in the target in our TTNY
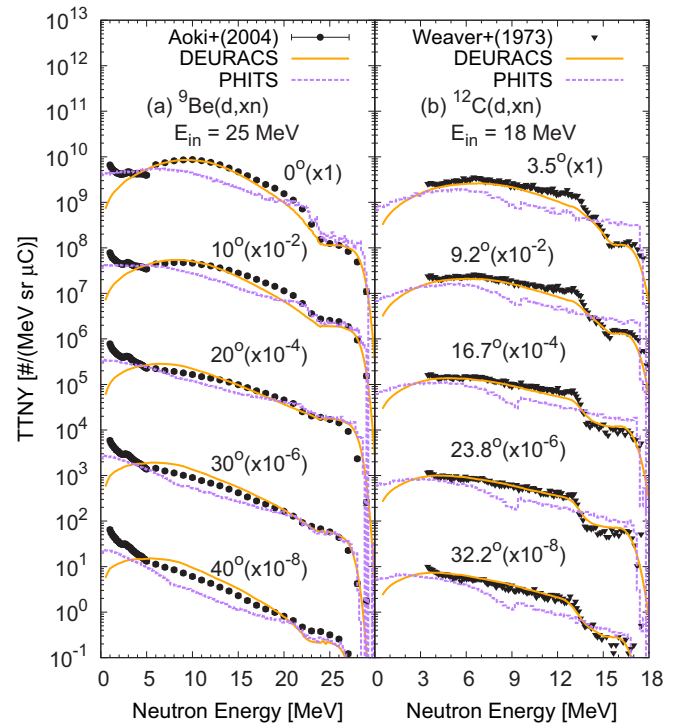
calculation was considered as one of possible causes for the underestimation.

However, the mean free path of multi-MeV neutrons in beryllium is estimated to be at least 2.7 cm, which is sufficiently longer than the thickness (3 mm) of the target used in the experiment [47]. Thus, the effect of multiple scattering is expected to be negligibly small. As shown in Figs. 5 and 6, the statistical decay is responsible for such low-energy neutron emission. Sequential particle decay from discrete levels in the residual light nuclei [e.g., $^9$Be$(E_x = 2.43$ MeV$)$] and unstable nuclei (e.g., $^5$He) is possible after the first chance particle emission via deuteron stripping and absorption reactions. Such neutron decay from discrete levels is not correctly taken into consideration in the CCONE code integrated in DEURACS. Enhancement in the low energy neutron yield is expected if a proper modification in the CCONE code is made.

## IV. SUMMARY AND CONCLUSION

We have analyzed double-differential thick target neutron yields (TTNYs) from deuteron bombardment on thick $^9$Be and $^{12}$C targets at incident energies up to 50 MeV and have investigated the involved reaction mechanism. The TTNYs were derived using the deuteron stopping power in the target and the double-differential $(d,xn)$ cross sections on $^9$Be and $^{12}$C calculated with the code system called deuteron-induced reaction analysis code system (DEURACS). The elastic breakup, proton stripping, and statistical decay

processes involved in the $(d,xn)$ reaction were taken into account by individual model codes integrated in DEURACS, namely, the CDCC, the Glauber plus DWUCK4, and the CCONE codes, respectively. The global nucleon and deuteron optical potentials and the widely used level density parameters were employed without any adjustment in the DEURACS calculation.

The calculated TTNYs reproduced the experimental data for incident energies up to 50 MeV quantitatively well over a wide range of neutron emission energy, excluding energies below a few MeV. Including our previous results of $(d,xp)$ reactions at 56 and 100 MeV, these results demonstrated the applicability of DEURACS to deuteron-induced reactions in the incident energy range up to 100 MeV. Also, the stripping processes were found to make the most dominant contribution to nucleon emission in the incident energy range of interest.

This suggests that modeling of the proton stripping reaction is essential to predict neutron production yields accurately in the design of deuteron accelerator neutron sources. The TTNY analysis also revealed that the DEURACS calculation underestimates production of low-energy neutrons. This is expected to be caused by the absence of sequential neutron emission from discrete levels of the residual nuclei. Further improvement of the statistical model code CCONE will be necessary as one of our future subjects.

[1] A. Moeslang, V. Heinzel, H. Matsui, and M. Sugimoto, Fusion Eng. Des. **81**, 863 (2006).

[2] M. Fadil and B. Rannou, Nucl. Instrum. Methods Phys. Res. B **266**, 4318 (2008).

[3] S. Agosteo, G. Curzio, F. d'Errico, R. Nath, and R. Tinti, Nucl. Instrum. Methods Phys. Res. A **476**, 106 (2002).

[4] Y. Nagai, K. Hashimoto, Y. Hatsukawa, H. Saeki, S. Motoishi, N. Sato, M. Kawabata, H. Harada, T. Kin, K. Tsukada, T. Sato, F. Minato, O. Iwamoto, N. Iwamoto, Y. Seki, K. Yokoyama, T. Shiina, A. Ohta, N. Takeuchi, Y. Kawauchi, N. Sato, H. Yamabayashi, Y. Adachi, Y. Kikuchi, T. Mitsumoto, and T. Igarashi, J. Phys. Soc. Jpn. **82**, 064201 (2013).

[5] T. Kin, Y. Nagai, N. Iwamoto, F. Minato, O. Iwamoto, Y. Hatsukawa, M. Segawa, H. Harada, C. Konno, K. Ochiai, and K. Takakura, J. Phys. Soc. Jpn. **82**, 034201 (2013).

[6] A. Boudard, J. Cugnon, J.-C. David, S. Leray, and D. Mancusi, Phys. Rev. C **87**, 014606 (2013).

[7] T. Sato, K. Niita, N. Matsuda, S. Hashimoto, Y. Iwamoto, S. Noda, T. Ogawa, H. Iwase, H. Nakashima, T. Fukahori, K. Okumura, T. Kai, S. Chiba, T. Furuta, and L. Sihver, J. Nucl. Sci. Technol. **50**, 913 (2013).

[8] S. Hashimoto, Y. Iwamoto, T. Sato, K. Niita, A. Boudard, J. Cufnon, J.-C. David, S. Leray, and D. Mancusi, Nucl. Instrum. Methods Phys. Res. B **333**, 27 (2014).

[9] Z. Wei, Y. Yan, Z. E. Yao, C. L. Lan, and J. Wang, Phys. Rev. C **87**, 054605 (2013).

[10] A. J. Koning, S. Hilaire, and M. Duijvestijn, *Proceedings of the International Conference on Nuclear Data for Science and Technology* (EDP Sciences, Les Ulis, 2008), p. 211.

[11] S. Nakayama, S. Araki, Y. Watanabe, O. Iwamoto, T. Ye, and K. Ogata, Nucl. Data Sheets **118**, 305 (2014).

[12] S. Nakayama, S. Araki, Y. Watanabe, O. Iwamoto, T. Ye, and K. Ogata, Energy Procedia **71**, 219 (2015).

[13] S. Nakayama and Y. Watanabe, J. Nucl. Sci. Technol. **53**, 89 (2016).

[14] S. Nakayama, H. Kouno, Y. Watanabe, O. Iwamoto, T. Ye, and K. Ogata, EPJ Web Conf. **122**, 04004 (2016).

[15] J. Lei and A. M. Moro, Phys. Rev. C **92**, 044616 (2015).

[16] G. Potel, F. M. Nunes, and I. J. Thompson, Phys. Rev. C **92**, 034611 (2015).

[17] B. V. Carlson, R. Capote, and M. Sin, Few-Body Syst. **57**, 307 (2016).

[18] J. F. Ziegler, M. D. Ziegler, and J. P. Biersack, Nucl. Instrum. Methods Phys. Res. B **268**, 1818 (2010).

[19] O. Iwamoto, J. Nucl. Sci. Technol. **44**, 687 (2007).

[20] O. Iwamoto, N. Iwamoto, S. Kunieda, F. Minato, and K. Shibata, Nucl. Data Sheets **131**, 259 (2016).

[21] M. Yahiro, K. Ogata, T. Matsumoto, and K. Minomo, Prog. Theor. Exp. Phys. **2012**, 1A206 (2012), and references therein.

[22] T. Ye, Y. Watanabe, and K. Ogata, Phys. Rev. C **80**, 014604 (2009).

[23] T. Ye, S. Hashimoto, Y. Watanabe, K. Ogata, and M. Yahiro, Phys. Rev. C **84**, 054606 (2011).

[24] J. Rayanl, *Proceedings of the Specialists' Meeting on the Nucleon Nucleus Optical Model up to 200 MeV* (OECD/NEA, Paris, 1997), p. 159.

[25] P. D. Kunz, computer code DWUCK4, University of Colorado (unpublished), http://spot.colorado.edu/~kunz/DWBA.html.

[26] K. Shibata, O. Iwamoto, T. Nakagawa, N. Iwamoto, A. Ichihara, S. Kunieda, S. Chiba, K. Furutaka, N. Otuka, T. Ohsawa, T. Murata, H. Matsunobu, A. Zukeran, S. Kamada, and J. Katakura, J. Nucl. Sci. Technol. **48**, 1 (2011).

[27] B. A. Watson, P. P. Singh, and R. E. Segel, Phys. Rev. **182**, 977 (1969).

[28] A. J. Koning and J. P. Delaroche, Nucl. Phys. A **713**, 231 (2003).

[29] D. G. Madland, *Proceedings of the Specialists' Meeting on Preequilibrium Nuclear Reactions* (OECD/NEA, Paris, 1988), p. 103.

[30] M. Kamimura, M. Yahiro, Y. Iseri, Y. Sakuragi, H. Kameyama, and M. Kawai, Prog. Theor. Phys. Suppl. **89**, 1 (1986).

[31] H. An and C. Cai, Phys. Rev. C **73**, 054605 (2006).

[32] A. Mengoni and Y. Nakajima, J. Nucl. Sci. Technol. **31**, 151 (1994).

[33] R. Capote, M. Herman, P. Oblozinsky, P. Young, S. Goriely, T. Belgya, A. Ignatyuk, A. Koning, S. Hilaire, V. Plujko, M. Avrigeanu, O. Bersillon, M. Chadwick, T. Fukahori, Z. Ge, Y. Han, S. Kailas, J. Kopecky, V. Maslov, G. Reffo, M. Sin, E. Soukhovitskii, and P. Talou, Nucl. Data Sheets **110**, 3107 (2009).

[34] X. D. Liu, M. A. Famiano, W. G. Lynch, M. B. Tsang, and J. A. Tostevin, Phys. Rev. C **69**, 064313 (2004).

[35] M. B. Tsang, J. Lee, and W. G. Lynch, Phys. Rev. Lett. **95**, 222501 (2005).

[36] S. G. Buccino and A. B. Smith, Phys. Lett. **19**, 234 (1965).

[37] Y. S. Park, A. Niiler, and R. A. Lindgren, Phys. Rev. C **8**, 1557 (1973).

[38] K. Miura, A. Sato, J. Takamatsu, S. Mori, Y. Takahashi, T. Nakagawa, T. Tohei, T. Niizeki, S. Hirasaki, G. C. Jon, K. Ishii, H. Orihara, and H. Ohnuma, Nucl. Phys. A **539**, 441 (1992).

[39] J. R. Davis and G. U. Din, Nucl. Phys. A **179**, 101 (1972).

[40] G. S. Mutchler, D. Rendic, D. E. Velkley, W. E. Sweeney Jr., and G. C. Phillips, Nucl. Phys. A **172**, 469 (1971).

[41] H. R. Schelin, E. F. Pessoa, W. R. Wylie, E. W. Cybulska, K. Nakayama, and L. M. Fagundes, Nucl. Phys. A **414**, 67 (1984).

[42] M. A. Kayumov, S. S. Kayumov, S. P. Krekoten, A. M. Mukhamedzhanov, K. D. Razikov, K. Khamidova, and P. Jarmukhamedov, Sov. J. Nucl. Phys. **48**, 403 (1988); EXFOR Entry No. A1301, dated 2012-04-06.

[43] K. Yoshida, T. Fukui, K. Minomo, and K. Ogata, Prog. Theor. Exp. Phys. **2014**, 53D03 (2014).

[44] N. Matsuoka, M. Kondo, A. Shimizu, N. Saito, S. Nagamachi, H. Sakaguchi, A. Goto, and F. Ohtani, Nucl. Phys. A **345**, 1 (1980).

[45] D. L. Smith, J. W. Meadows, and P. T. Guenther, Nucl. Instrum. Methods Phys. Res. A **241**, 507 (1985).

[46] M. A. Lone, C. B. Bigham, J. S. Fraser, H. R. Schneider, T. K. Alexander, A. J. Ferguson, and A. B. McDonald, Nucl. Instrum. Methods **143**, 331 (1977).

[47] T. Aoki, M. Hagiwara, M. Baba, M. Sugimoto, T. Miura, N. Kawata, and A. Yamadera, J. Nucl. Sci. Technol. **41**, 399 (2004).

[48] M. J. Saltmarsh, C. A. Ludemann, C. B. Fulmer, and R. C. Styles, Nucl. Instrum. Methods **145**, 81 (1977).

[49] J. P. Meulders, P. Leleux, P. C. Macq, and C. Pirart, Phys. Med. Biol. **20**, 235 (1975).

[50] Y. Tajiri, Y. Watanabe, N. Shigyo, K. Hirabayashi, T. Nishizawa, and K. Sagara, Prog. Nucl. Sci. Technol. **4**, 582 (2014).

[51] K. A. Weaver, J. D. Anderson, H. H. Barschall, and J. C. Davis, Nucl. Sci. Eng. **52**, 35 (1973); EXFOR Entry No. F0218, dated 2013-06-04.

[52] K. Shin, K. Hibi, M. Fujii, Y. Uwamino, and T. Nakamura, Phys. Rev. C **29**, 1307 (1984).

[53] G. Lhersonneau, T. Malkiewicz, K. Kolos, M. Fadila, H. Kettunen, M. G. Saint-Laurent, A. Pichard, W. H. Trzaska, G. Tyurin, and L. Cousin, Nucl. Instrum. Methods Phys. Res. A **603**, 228 (2009).

[54] G. W. Schweimer, Nucl. Phys. A **100**, 537 (1967).

[55] Z. Radivojevic, A. Honkanen, J. Äystö, V. Lyapin, V. Rubchenya, W. H. Trzaska, D. Vakhtin, and G. Walter, Nucl. Instrum. Methods Phys. Res. B **183**, 212 (2001).